


Submission to IWMPPI 2022

# Image Time-Series Stability for MPI-Based Functional Neuroimaging

John M. Drago <sup>a,b,\*</sup>, Erica E. Mason <sup>b</sup>, Eli Mattingly <sup>b,c</sup>, Monika Śliwiak <sup>b</sup>, Lawrence L. Wald <sup>b,c</sup>

<sup>a</sup>Department of Electrical Engineering and Computer Science, MIT, Cambridge, MA, USA

<sup>b</sup>Martinos Center for Biomedical Imaging, Massachusetts General Hospital, Boston, MA, USA

<sup>c</sup>Harvard-MIT Health Sciences and Technology, Cambridge, MA, USA

\*Corresponding author, email: jdrago@mit.edu

© 2021 Drago et al.;

## Abstract

The temporal stability of an image time-series becomes a critical performance metric when magnetic particle imaging (MPI) is used as a functional neuroimaging modality. We apply an existing framework for assessing time-series variance from the functional MRI (fMRI) literature to phantom MPI time-series images. In this framework, sources of time-series variance are divided into those arising from thermal noise sources (which do not scale with the signal level) and intensity variations that scale with the signal level. The latter are often thought of as “physiological noise” if they arise from physiological processes or as instrumental “nuisance fluctuations” when arising from instrumental instabilities, such as system gain fluctuations. We analyze the phantom imaging time-series stability of a rodent-sized field-free line (FFL) MPI scanner and assess the relative contributions of different noise sources to the time-series by varying the super-paramagnetic iron-oxide nanoparticle (SPION) concentration. These measurements permit characterization of our system’s time-series noise and suggest the signal levels at which the time-series will be dominated by instrumental instabilities rather than thermal noise or physiological modulations.

## I. Introduction

Cerebral blood volume (CBV)-based functional neuroimaging modalities attempt to detect the approximate 20% blood volume changes that occur during neural activation [1]. Within this abstract, we describe a framework (from the fMRI literature) for time-series signal-to-noise ratio (SNR) metric quantification in MPI-based functional neuroimaging. We additionally demonstrate phantom imaging time-series stability and characterize the thermal and instrumental instability contributions for our existing small-animal imaging system.

### I.1. The tSNR Formulation

The ratio of a pixel’s signal level to its intensity variation across a time-series of images is the principal signal-to-noise metric for time-series functional neuroimaging

experiments. Following the terminology and analysis of Kruger and Glover [2], this metric, termed “tSNR”, is formed from the ratio of the pixel’s mean intensity,  $\bar{S}$ , to its standard deviation over time, defined as  $\sigma_{\text{total}}$ .

$$\text{tSNR} = \frac{\bar{S}}{\sigma_{\text{total}}} \quad (1)$$

In *in vivo* functional neuroimaging, “noise” in the time-series arises from both thermal noise,  $\sigma_0$ , and from noise sources whose variation increases in proportion to the signal. Signal-level-dependent noise sources include instrument instabilities with this signal dependence and physiological signal modulation, and they are collectively termed “physiological noise”,  $\sigma_p$  [3].

The SNR of an individual image due only to thermal noise,  $\sigma_0$ , is defined:

$$\text{SNR}_0 = \frac{\bar{S}}{\sigma_0} \quad (2)$$

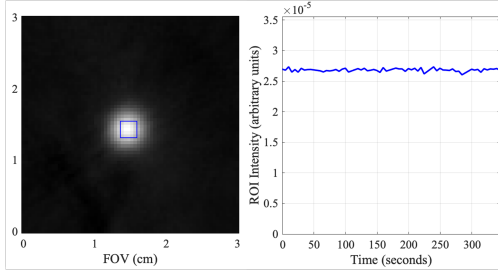


**Figure 1:** An example ROI for an 18  $\mu\text{l}$  spherical glass bulb phantom with 5  $\mu\text{g}$  Fe/ml Synomag®-D, and the mean of this ROI over the five-minute time-series with an image acquired every five seconds.

Here,  $\sigma_0$  is of thermal origin from coil or body losses or preamplifier noise.  $\sigma_p$  should ideally reflect signal modulation from physiological processes (such as respiration and cardiac activity). If these two “noise” sources are thought to be uncorrelated, then we can define the total time-series image noise,  $\sigma_{\text{total}}$  [2]:

$$\sigma_{\text{total}} = \sqrt{\sigma_0^2 + \sigma_p^2}. \quad (3)$$

The determination of the ratio of physiological noise to thermal noise can be derived by comparing measurements of  $\text{SNR}_0$  and tSNR.

$$\frac{\sigma_p}{\sigma_0} = \sqrt{\left(\frac{\text{SNR}_0}{\text{tSNR}}\right)^2 - 1} \quad (4)$$

When  $\sigma_p$  can be described as a modulation of the signal, it is proportional to the signal level:  $\sigma_p = \lambda \bar{S}$ , with proportionality constant,  $\lambda$ . A direct relationship between  $\text{SNR}_0$  and tSNR can then be formed.

$$\text{tSNR} = \frac{\text{SNR}_0}{\sqrt{1 + (\lambda \text{SNR}_0)^2}} \quad (5)$$

Equation 5 describes a system where the tSNR does not increase indefinitely as  $\text{SNR}_0$  is improved, but approaches an asymptotic value of  $1/\lambda$ , as the image SNR ( $\text{SNR}_0$ ) increases. Similar to the biological sources, instrumental gain variations over time could also contribute signal-level-dependent “noise” to phantom image time-series. It is desirable for these non-thermal instrumental variances to be insignificant compared to the unavoidable biological and thermal sources. When instrumental modulations that are proportional to  $\bar{S}$  are small,  $\lambda$  is near zero for phantom imaging, and the plot of tSNR vs.  $\text{SNR}_0$  should be the identity line.

Operation of the scanner in a regime maximally sensitive to biological sources is especially important given that some biological sources are of interest. For example, metabolic fluctuations from neuronal firing, whose correlations form the basis of brain network analysis is a source of physiological noise. Physiological time-series

variance that is proportional to signal level has been previously reported in resting rodent brain MPI signals [4], which is consistent with neuronal-driven CBV fluctuations. An instrumentation goal, therefore, is to create a time-series scanner whose  $\lambda$  in phantom data is sufficiently smaller than the expected  $\lambda$  value for *in vivo* measurements. This would ensure that a given MPI system is capable of detecting the physiological “noise” of interest. We demonstrate the characterization of the  $\lambda$  free parameter for our system below.

## II. Methods

The small-animal imager used for tSNR characterization has been detailed previously [5, 6]. The image resolution for this 2.83 T/m, mechanically-rotating FFL system is approximately 2.5 mm. A five-second image is formed from 27 projections, spanning 180 degrees. Sixty-six projection points are acquired at each angle to span a field of view of 30 mm. Image reconstruction was performed with an inverse Radon transform algorithm implemented on MATLAB (Mathworks, Natick, MA).

Multiple 18  $\mu\text{l}$  glass bulbs phantoms were filled with PEG-coated 70 nm Synomag®-D (micromod, Germany) diluted in deionized water. Phantoms with iron concentrations spanning three orders of magnitude were used. The iron concentrations roughly reflect the expected *in vivo* concentrations of a rodent brain. If a 300 g rodent is injected with a 10 mg Fe/kg SPION dose, assuming rodent total blood volume of 64 ml/kg with 5% voxel blood volume [4], we expect a concentration of 7.88  $\mu\text{g}$  Fe/ml in the brain. Thus, sensitivity to 1.6  $\mu\text{g}$  Fe/ml is needed to detect a 20% blood volume change.

A 60-image time-series, comprised of five minutes of continuous, five-second images, was acquired for each imaging run. Following standard functional neuroimaging post-processing, a third-degree polynomial was fit to the acquired data, and low temporal frequency signal drift was removed from the time-series [7, 8]. To quantify the thermal noise that defines  $\sigma_0$ , the standard deviation of an individual pixel was taken across all time points with no SPIONs in the imaging bore.  $\sigma_{\text{total}}$  and  $\bar{S}$  are measured by taking the standard deviation and mean, respectively, of a given pixel across the time-series. Metrics were averaged over a  $5 \times 5$  pixel grid in the center of the glass bulb (Figure 1). The free parameter,  $\lambda$ , was determined by using a nonlinear solver in MATLAB to fit the resultant tSNR and  $\text{SNR}_0$  data to Equation 5.

## III. Results

Figure 1 shows an example plot of the region of interest (ROI) mean over the time-series. Figure 2 shows a plot of  $\text{SNR}_0$  as iron concentration increases. The plot exhibits the expected linear increase in signal as the iron

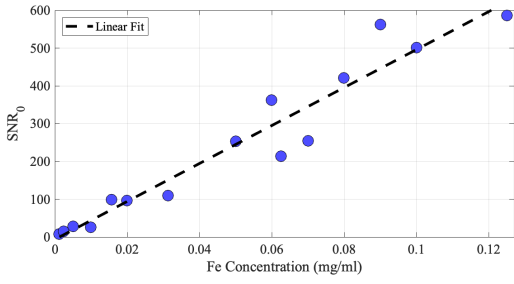


**Figure 2:**  $\text{SNR}_0$  in a  $5 \times 5$  phantom ROI vs. iron concentration.  $\text{SNR}_0$  increases, as expected, with the concentration of iron. The  $R^2$  for the plotted data, assuming a linear fit, is 0.93.

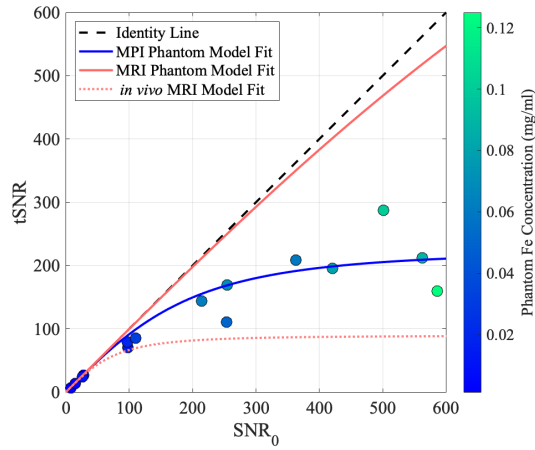


**Figure 3:** Plot of  $\text{tSNR}$  as  $\text{SNR}_0$  increases. The  $\lambda$  parameter for the evaluated small-bore MPI phantom imaging system was  $\lambda = 0.00444$ . From MRI phantom measurements in the literature [3],  $\lambda = 0.00075$  (red solid line), and from *in vivo* fMRI imaging,  $\lambda = 0.0112$  (red dashed line).

concentration is increased. The resultant  $\text{tSNR}$  vs.  $\text{SNR}_0$  plot for the phantom measurements is shown in Figure 3. Each point in the plot represents a different iron concentration, as indicated in the color bar. The  $\lambda$  determined by fitting Equation 5 to the measured data was 0.00444. Figure 3 demonstrates this model fit as a solid blue line.

## IV. Discussion and Conclusion

We formalize and apply a framework to characterize the temporal stability of functional MPI (fMPI) systems. From the fMRI literature, the value of  $\lambda$  has been shown to change based on the imaging system used (e.g., 1.5 T vs. 3 T vs. 7 T), but the parameter value of  $\lambda$  for *in vivo* functional imaging is typically around  $\lambda = 0.010$ , whereas for a phantom,  $\lambda$  is on the order of  $10\times$  lower:  $\lambda = 0.0008$  [3]. The derived  $\lambda$  value from phantom imaging of our MPI system is 0.00444 – a higher instrumentation variation source than what is observed in fMRI. It will be important to determine whether different SPIONs produce varying

$\lambda$  values in phantom and *in vivo* imaging.

From Equations 4 and 5, the expected  $\text{SNR}_0$  value that corresponds to a 1:1 ratio of  $\sigma_0$  to  $\sigma_p$  in our system for phantom imaging was determined to be  $\text{SNR}_0 = \frac{1}{\lambda} = 225$ . For image SNR below this, sources of noise other than signal-level-dependent instrumental instabilities are expected to dominate. The *in vivo* SPION concentration for rodent imaging is expected to be on the order of  $10 \mu\text{g Fe/ml}$ , which corresponds to a phantom  $\text{SNR}_0$  of approximately 26 in our system. At this  $\text{SNR}_0$ , the  $\sigma_p$  to  $\sigma_0$  ratio from instrumental sources is expected to be 11.5%. This ratio demonstrates that  $\text{tSNR}$  will be dominated by either thermal noise or genuine physiological fluctuations for our current imaging system at the expected *in vivo* SPION concentration and not by signal-level-dependent noise instabilities in the instrument. This motivates the use of the current system in rodent fMPI studies to characterize the noise contribution from physiological processes with *in vivo* rodent testing and ultimately determine the asymptotic limit of  $\text{tSNR}$  that can be achieved with *in vivo* brain fMPI.

## Author's Statement

Authors state no conflict of interest.

## References

- [1] T. Kim, K. S. Hendrich, K. Masamoto, and S.-G. Kim. Arterial versus total blood volume changes during neural activity-induced cerebral blood flow change: Implication for bold fmri. *Journal of Cerebral Blood Flow & Metabolism*, 27(6):1235–1247, 2007.
- [2] G. Krüger and G. H. Glover. Physiological noise in oxygenation-sensitive magnetic resonance imaging. *Magnetic Resonance in Medicine: An Official Journal of the International Society for Magnetic Resonance in Medicine*, 46(4):631–637, 2001.
- [3] C. Triantafyllou, R. D. Hoge, G. Krueger, C. J. Wiggins, A. Potthast, G. C. Wiggins, and L. L. Wald. Comparison of physiological noise at 1.5 t, 3 t and 7 t and optimization of fmri acquisition parameters. *Neuroimage*, 26(1):243–250, 2005.
- [4] C. Z. Cooley, J. B. Mandeville, E. E. Mason, E. T. Mandeville, and L. L. Wald. Rodent cerebral blood volume (cbv) changes during hypercapnia observed using magnetic particle imaging (mpi) detection. *NeuroImage*, 178:713–720, 2018.
- [5] K. Herb, E. Mason, E. Mattingly, J. Mandeville, E. Mandeville, C. Cooley, and L. Wald. Functional mpi (fmpi) of hypercapnia in rodent brain with mpi time-series imaging. *International Journal on Magnetic Particle Imaging*, 6(2 Suppl 1), 2020.
- [6] E. Mattingly, E. Mason, K. Herb, M. Śliwiak, K. Brandt, C. Cooley, and L. Wald. Os-mpi: An open-source magnetic particle imaging project. *International Journal on Magnetic Particle Imaging*, 6(2 Suppl 1), 2020.
- [7] A. M. Smith, B. K. Lewis, U. E. Ruttimann, Q. Y. Frank, T. M. Sinnwell, Y. Yang, J. H. Duyn, and J. A. Frank. Investigation of low frequency drift in fmri signal. *Neuroimage*, 9(5):526–533, 1999.
- [8] R. Kopel, R. Sladky, P. Laub, Y. Koush, F. Robineau, C. Hutton, N. Weiskopf, P. Vuilleumier, D. Van De Ville, and F. Scharnowski. No time for drifting: Comparing performance and applicability of signal detrending algorithms for real-time fmri. *NeuroImage*, 191:421–429, 2019.